Rapid quench piston cylinder apparatus: an improved design for the recovery of volatile-rich geological glasses from experiments at 0.5-2.5 GPa

Isra S. Ezad[1*], Svyatoslav S. Shcheka[1], Stephan Buhre[2], Andreas Buhre[3], Lauren R. Gorovjovsky[1], Joshua J. Shea[1], Michael W. Förster[1,4], Stephen F. Foley[1,4]

[1]School of Natural Sciences, Macquarie University, North Ryde, Sydney, NSW, 2109, Australia

[2]Institute of Geosciences, Johannes Gutenberg University Mainz, Mainz, Germany

[3]GUKO Sondermaschinenbau GmbH**,** Am Mühlensiek 4, 37170 Uslar, Germany

[4] Research School of Earth Sciences, Australian National University, Canberra, ACT, 2601, Australia

*corresponding author: isra.ezad@mq.edu.au

This is a **non-peer reviewed preprint manuscript** submitted to EarthArXiv on 6 October 2022. This manuscript has been **submitted for publication to Reviews of Scientific Instruments**. Please note this manuscript had not yet undergone peer-review and, as such, the final version of this manuscript may have changes and will be available via the peer-reviewed publication DOI, if accepted

Abstract

The accurate and precise determination of the compositions of silicate glasses formed from melts containing the volatile components H_2O and CO_2 recovered from high-pressure, high-temperature experiments is essential to our understanding of geodynamic processes taking place within the planet. Silicate melts are often difficult to analyse chemically because the formation of quench crystals and overgrowths on silicate phases is rapid and widespread upon quenching of experiments, preventing the formation of glasses in low-SiO_2 and volatile-rich compositions.

Here, we present experiments conducted in a novel rapid quench piston cylinder apparatus on a series of partially molten low-silica alkaline rock compositions (lamproite, basanite, calk-alkaline basalt) with a range of water contents. Quench modification of the volatile-bearing silicate glasses is significantly reduced compared to those produced in older piston-cylinder apparatuses. The recovered glasses are almost completely free of quench modification and facilitate the determination of precise chemical compositions. We illustrate the significantly improved quench textures and provide an analytical protocol that recovers accurate chemical compositions from both poorly and well-quenched silicate glasses.

Introduction

Experimental petrology has advanced our understanding of the planet's interior by allowing access to the pressures and temperatures of formation and equilibration of rocks. The success of experimental petrology has relied on the continued development of high-pressure, high-temperature techniques including internally heated pressure vessels, piston cylinder and multi-anvil apparatuses, and diamond-anvil cells (Boyd and England, 1960; Kawai and Endo, 1970; Walker et al., 1990). These high-pressure techniques are now able to investigate conditions up to 500 GPa, covering the entire pressure-temperature space within the Earth and other planetary bodies (Ishii et al., 2019; Jenei et al., 2018; Masotta et al., 2012).

Melting within the Earth's mantle is restricted largely to a "magmatic zone" at depths between 40 and 250km (Foley and Pintér, 2018), with most melting occurring in the

uppermost 140km (equivalent to ≈ 4.4 GPa). This makes piston-cylinder apparatuses especially useful due to their pressure range (0.5–4.0 GPa) and excellent temperature control.

The characterisation of melt compositions by analysing quenched glasses from experiments has led to a good understanding of fairly dry melt compositions derived from the mantle and crust, but the addition of water leads to the rapid, uncontrolled and abundant growth of crystals, both as individual crystals and as overgrowths on equilibrium crystals, during the short quenching period between run temperature and the solidus of the rock. This quench modification can falsify melt compositions considerably due to the growth of thin rims around minerals (Green, 1976), and little glass may remain to analyse in water-rich, and particularly CO_2-rich, experiments. During the quenching of an experiment the inevitable contraction of the capsule assembly usually leads to a pressure drop and may lead to the formation of low-pressure phases that are not stable at nominal run conditions.

Uncertainties surrounding the interpretation of quench textures has fuelled considerable controversy around the identification of equilibrium crystals, melts, and fluids in water-rich experiments, which carry over into the interpretation of melting points and melt compositions (Grove et al., 2006; Till et al., 2012; Green et al., 2014). These problems are especially relevant to low-SiO_2 alkaline silicate melts with low viscosities and depolymerised melt structures (Hess, 1977; Mysen et al., 1982) such as nephelinites, basanites, melilitites and lamproites, which have long been known to require H_2O in their source regions, so that no meaningful models for their origin can be drawn from dry experiments.

Many igneous melts are thought to require mixed COH volatiles, either as H_2O+CO_2 in relatively oxidised conditions or H_2O+CH_4 in more reduced natural conditions (Green and Falloon, 1998), which further complicate quenching behaviour. Here, we concentrate on the investigation of quenching behaviour in water-bearing melts and glasses and include a comparison with mixed H_2O+CH_4 volatiles, but do not consider H_2O+CO_2 mixtures.

Several intricate, time-consuming and expensive methods have been introduced in an attempt to better characterise the compositions of high-pressure melts. These include: [1] a series of “sandwich” experiments in which the analysed melt composition is run in additional experiments together with its source rock (Wallace and Green, 1988; Davis et

al., 2011); [2] Melt traps consisting of vitreous carbon or diamond that separate the melt from the rock during the experiment and before the quenching procedure (Hirose and Kushiro, 1993); and [3] volume integration of microprobe analyses achieved by re-polishing and analysing several levels through quenched melt pockets (Pintér et al., 2021).

However, these methods have circumvented the quench issue rather than attempting to solve it. Here, we introduce a novel rapid quench piston cylinder apparatus (RQPC) which improves the preservation of melts as glasses by increasing the rate of temperature reduction immediately after turning off the heating of the experiments.

We demonstrate that the RQPC produces better quenched glasses for a series of low-SiO_2 rock compositions with added water that are directly relevant to the origin of alkaline rocks. This obviates the need for the expense of multiple experiments and complicated experimental designs. We present results for tests of the RQPC using anhydrous and hydrous silicate melts and compare the results to those from traditional end-loaded piston cylinder apparatuses.

Experiments and analytical methods

The GUKO rapid quench piston cylinder apparatus: technical aspects

The rapid-quench piston-cylinder apparatus manufactured by GUKO Sondermaschinen–bau GmbH, Uslar, Germany, is installed in the School of Natural Sciences at Macquarie University, Sydney, Australia. Major design changes relative to traditional piston-cylinder apparatuses (Boyd and England, 1960) include a 2.4 megaNewton lightweight frame consisting of several plates rather than a single massive steel frame (Figure 1a,b), a novel pressure control stabilization, and a heating controller 10 time faster than Eurotherm. The rapid quench facility is supported by the use of internally cooled half-inch Strecon® pressure vessels (Figure 1d). Twelve extra vertical cooling channels around the tungsten core draw heat away radially from the tungsten carbide core, reducing thermal gradients along the furnace axis. Along with massive coolers (and circulation of a pre-cooled water/glysantin® mix) connected to the hydraulic bridge and top plate. This results in more rapid cooling of the sample and also prolongs the lifetime of the core. Pressure and temperature controls are fully integrated into a powerful Siemens SPS system.

A novel pressure control system was developed to compensate instantly for any volume change inside the pressurized volume. This is achieved by a constant oil stream bypassing the primary end of the pressure intensifier. In this setup the displacement of the hydraulic cylinders does not affect the prevailing pressure.

Calibration of the rapid-quench piston-cylinder apparatus

Calibration of pressure and temperature in the GUKO RQPC is similar to that in other piston-cylinder apparatuses and all experiments were performed using an assembly with natural CaF_2 as pressure-transmitting medium (Figure 2), with MgO spacers and a standard graphite heater. These internal parts are not yet optimized for rapid quench, so that further improvements are possible. Temperature was monitored with Type B ($Pt_{30}Rh_{70}$–Pt_6Rh_{94}) thermocouples placed directly above the sample, and pressure was calibrated using the albite = jadeite+quartz reaction (Holland, 1980).

Experimental tests of quenching ability

We have tested the ability of the GUKO rapid-quench piston-cylinder apparatus (RQPC) to produce well-quenched experimental run products with a series of experiments on low-SiO_2 and alkaline melt compositions with different water contents and compare results to equivalent experiments in older piston-cylinder apparatuses.

The starting materials include three synthetic oxide mixtures and three powdered natural rock samples; the compositions of which are presented in Table 1. Three (GL, LL and LC) are potassic compositions, one is a basanite (BK-75115) and the others a tholeiitic basalt and a calk-alkaline dacite. The purpose of producing well-quenched glasses in the experiments differed, and included (i) the optimisation of mineral/melt partition coefficients in lamproite melts (Ezad and Foley., in press), and (ii) synthetic calc-alkaline and basaltic silicate glasses were used to test the solubility of sulfur species in basaltic melts at varying fO_2 conditions. These experimental applications require precise and accurately determined chemical compositions of melts in equilibrium with their surrounding mineral phases and were therefore ideal projects to test improvement of the rapid quenching ability of the GUKO press relative to earlier apparatuses.

All experiments used the same natural CaF_2 assemblies and thermocouples as in the calibration experiments (Figure 2). Capsule design varied between experimental projects to allow for flexibility from running several compositions in the same experiment, to

ensuring fluid was not lost during the generation of hydrous melts with added free water. Capsule configurations are described in Table 2. Graphite capsules with dual sample chambers wrapped in 25μm Pt foil were used for calc-alkaline and basaltic silicate glasses, whereas welded Pt capsules enriched in iron to minimise further iron loss were used for mineral/melt partitioning experiments (Ezad and Foley, in press).

Experimental runs are automated by the GUKO-software (Figure 1c), with which users are able to program complex "recipes" consisting of several ramps and ramping rates for compression and heating, hold for specified durations, quenching and decompression. Quenching to room temperature from temperatures of 1300°C is achieved in 10 seconds once power is cut to the transformer. The advantage of the GUKO RQPC lies in the extra cooling power in combination with internally cooled Strecon® pressure vessels, which facilitate more rapid initial cooling from run temperature to sub-solidus temperatures.

For experiments designed to determine mineral/melt partition coefficients, experimental charges were first brought to the desired pressure before being rapidly heated at 41°C per minute to above-liquidus conditions, and then slowly cooled at a rate of 10°C per minute until the final run temperature was achieved. This optimises the growth of a few large crystals that can more easily be analysed for trace elements by Laser-ICP-MS or SIMS by initiating crystallisation in conditions with low nucleation rates (Tiepolo et al., 2000). Experiments typically lasted 15 - 24 hours to ensure the growth of large primary minerals including phlogopite and olivine, after which they were quenched to room temperature. Full results of the partitioning study are given in Ezad and Foley (in press).

The experiments presented here allow several comparisons of the quenchability of melts to be made: the calk-alkaline dacite and tholeiitic basalts were run with and without added water, and basanite (BK-75115) and a low-SiO_2 lamproite (LC) were run with added water to widen the compositional scope of melts studied.

The SiO_2-richer Gaussberg lamproite composition (GL and LL) was used to compare quench textures with experiments conducted in older piston-cylinder apparatuses. The fluid-saturated experiment T-1863 was conducted in Tasmania with a mixed H_2O+CH_4 fluid under reducing conditions in a Boyd-England end-loaded ½" piston cylinder apparatus. The fluid was analysed by GCMS as 80% H_2O (Foley, 1989; Taylor and Foley, 1989) but the amount of H_2O in the melt is not known (but surely higher than other experiments reported here). Further, an additional experiment (OLD-PC 212; Table 2)

was performed. also using a Boyd and England-type end-loaded ½" piston cylinder apparatus at Macquarie University with the same lamproite composition (GL in Tables 1 and 2) as in Ezad and Foley (in press) and Foley (1989). Run conditions for all experiments are presented in Table 2.

Analytical methods

All samples recovered from high-pressure experiments were sliced using a diamond wire saw to expose the sample, after which capsules were embedded in epoxy resin and polished to a 1μm diamond finish.

High-resolution imaging was conducted at Macquarie University using an FEI – Field Emission Scanning Electron Microscope (FE-SEM) operating at 15 kV, 11 nA beam current, calibrated to specimen current of 13 nA using a Faraday cup on the sample stage, with a spot size of 14.8 μm and a working distance of ~10 mm. Example BSE images are shown in Figures 3, 5 and 6.

Chemical compositions of melts were quantitatively determined by wavelength-dispersive spectroscopy (WDS) using a 5 spectrometer Field Emission Electron Micro Probe Analyser (FE-EMPA) JEOL JXA 8530F at the University of Tasmania, operating at 15 kV and 10 nA. Acquisition positions were selected by pre-programming positions on glasses with a minimum of 5 analyses per sample; a defocussed beam was used on all experimental charges with a spot size of 10-20 μm to minimise beam damage and alkali loss. Times for the acquisition of background were also adjusted to minimise beam damage and improve detection of minor elements at low concentrations; 10/10s respectively was used for Ca; 20/20 for Mg, Si, K, Na, Ti, Mn, Fe, Cl, Cr, Ba, Ni; 40/40 for P, and 70:70 for F.

Experimental charges from traditional piston cylinder apparatuses have texturally complex quenched glass mats (Figure 3 a-d) and contain quenched minerals including phlogopite and other minor phases. Despite the challenging texture, FE-EMPA measurements were acquired using a large 20 μm defocussed beam to homogenise the quenched regions in a grid covering an area of 100 μm^2.

Additional high-resolution imaging and chemical characterisation of a single high-pressure experiment recovered from the RQPC was conducted by Photo-induced Force Microscopy (PiFM) (Otter et al., 2021) at the Research School of Earth Sciences,

Australian National University. PiFM combines atomic force microscopy with infrared spectrometry, allowing for the collection of FTIR maps at sub-micron scale. PiFM maps were acquired on a small 256 x 256 pixel area at known infra-red wavenumbers chosen to correspond to the ν_3 stretching vibration of C-O of carbonate (1450 cm^{-1}) and the ν_3 stretching vibration of Si-O of silicate melt (1150 cm^{-1}) and mica (1000 cm^{-1}) (Figure 4).

Results

The size of quench crystals and the textures and homogeneity of glasses in experimental run products from both RQPC experiments and those from older piston-cylinder apparatuses is illustrated in Figures 3 to 6.

Figure 3 depicts run products on the same rock compositions, but with different volatile mixes and in different apparatuses. The starting composition for each of these experiments was a hydrous synthetic leucite lamproite based on lavas of the Gaussberg volcano in eastern Antarctica. The RQPC experiment M21-059 (Figure 3e-f) was designed to constrain partition coefficients between minerals and the melt (presented in Ezad and Foley, in press). Experiment T-1863 (Figure 3a-b) was conducted at the University of Tasmania in the mid 1980s and is a fluid-saturated run with a mixed fluid consisting of 80% H_2O and 20% CH_4 (Foley, 1989). Experiment OLD-PC 212 (Figure 3c-d) is a control run in an old piston-cylinder apparatus at Macquarie University with the same starting materials and water content as in M21-059: the only difference between the experiments is quench duration, with the rapid quench reaching ambient temperature much more quickly. Figures 3c-f show the stark difference in quenched glass texture, with quench crystals reduced in size by an order of magnitude in the RQPC. Experiments conducted using the rapid quench piston cylinder have large regions of silicate glass which appear to be quench-free (Figure 3c). Only at high magnification (x 6500) are small quench needles on the order of 1 micrometre visible.

PiFM maps (Figure 4) show that tiny (200 nm) quenched phlogopite and calcite are the only phases present in the glass in the hydrous lamproite experiment from the RQPC (M21-059). Despite the imaging of quenched phlogopites using FE-SEM, the 200nm long and <40nm wide calcite quench crystals were not identified until PiFM maps were collected. This indicates that volatiles are not lost during quenching and that the use of

large defocused beams is essential to ensure these small phases are reconciled within glass compositions to arrive at an accurate, homogenised melt composition.

Figure 5 compares BSE images of RQPC run products with different rock compositions and different water contents, each together with a high magnification image of a small glass area shown by the white rectangles. Figure 5a-b shows an experiment on the low-SiO_2 Lake Cargelligo lamproite with high CaO (9.5 wt%), MgO (13.5 wt%) and 3 wt% H_2O. These are compared to a dry calc-alkaline dacite (66.5 wt% SiO_2, 1.2 wt% MgO; Figure 5c-d) and a basanite (41.5 wt% SiO_2, 11.7 wt% MgO) with 10 wt% added H_2O (Figure 5e-f). The exceptionally well-quenched glass in the dacite is expected for SiO_2-rich and dry compositions (Figure 5c-d) and known from many experimental studies (Melekhova et al., 2017; Parat et al., 2014), whereas a similarly well-quenched glass from an alkaline, low-SiO_2 composition with 3wt% H_2O (Figure 5a-b) is made possible by the RQPC. The higher H_2O content (10 wt%) in the low-SiO_2 basanite leads to discernible quench crystals even in the RQPC, but these are only 2-3µm long (Figure 5e-f). This is a major improvement over the large, continuous, and heterogeneously distributed mats of quench crystals from water-rich experiments conducted in traditional piston cylinder apparatuses (Figure 3a-b). Quench phases in these experiments are tens of micrometres across and cause falsified glass compositions (Green, 1976), making accurate chemical analysis almost intractable.

Figure 6 illustrates the quench products in further experiments on a tholeiitie basalt with and without water and the dacite with 5% added H_2O. The tholeiite quenches well to a glass both when dry (Figure 6a-b) and with added water (Figure 6e-f); the highly reflective sulphide minerals are more dispersed and smaller in the hydrous experiment (Figure 6f vs. 6b) but the glass in the background contains no discernible quench crystals. The dacite containing 5 wt% H_2O (Figure 5c-d) quenches to a glass as good as the dry experiment on the same composition (Figure 3d).

Analysis of melt compositions

Volatile-rich melts generally quench poorly in piston-cylinder experiments, leading to various textures such as quench overgrowths on equilibrium crystals to complex mats of interlocked larger crystals, particularly when mixed volatile species are used (e.g. Figure 3a). For the analysis of melt compositions, the dramatic improvement in quench textures in the RQPC allow direct analysis of well-quenched glasses, which is preferable to

elaborate systems of analysis such as area analysis, averaging of numerous analytical points using defocussed microprobe beams, or re-polishing and re-analysis.

Chemical compositions for the experimental glasses are reported in Table 3 and can be compared to the starting compositions in Table 1; the latter were obtained for the natural starting materials by XRF major element analysis of whole rock powders prior to high-pressure, high-temperature experiments. This provides an independent quantitative check for melt compositions analysed in the rapid quench piston cylinder. The quench crystal-free glasses in the synthetic dacite and tholeiite compositions (Figures 6) are successfully reproduced by rapid quenching of the glasses (Table 3), showing consistent reproducibility across several high-pressure experiments. The quality and reproducibility of the analyses is high for water-bearing experiments, exemplified by basanite run A21-104B, which shows standard deviations less than the uncertainty of the microprobe for elements other than Na (Table 3).

Similar comparisons for the series of lamproite experiments are less clearly defined, as the mineral phases phlogopite, clinopyroxene and/or olivine grew during the partitioning experiments so that the melts reflect fractionated compositions that do not correspond to the whole experimental charge.

However, a glassing experiment with only melt and 5wt% H_2O from the old Macquarie piston cylinder apparatus (OLD-PC-212) can be compared to A21-063 a glass-only experiment to which no additional water was added in the RQPC (Table 4). Despite the visibly coarser grained quench texture produced by the traditional piston cylinder apparatus (Figure 3d) the compositions determined by EPMA are similar, with the largest deviations between the two compositions in SiO_2 (1.76 wt% difference), Al_2O_3 (0.74 wt%) and CaO (2.1 wt%). For all other major elements, the difference between the two experimental glasses is less than 0.5 wt%. Whilst not insignificant, the small differences between the two glass compositions fall within the standard deviations determined from the individual EMPA WDS measurements, suggesting that a careful EMPA approach to homogenising glass compositions determined from quench products is satisfactory in reproducing accurate chemical compositions also in older piston-cylinder experiments.

Our experiments demonstrate that whilst analysing complex quench textures remains analytically challenging, the compositions determined by homogenising large areas are

robust and representative of the "true" composition when compared to clearly "cleaner" and therefore analytically simpler glasses produced by the RQPC.

Implications

We present the first experimental results comparing the structure and composition of quenched melts between a new "rapid quench" piston cylinder apparatus and traditional piston cylinder apparatuses. Our preliminary findings demonstrate quenching rates of less than 10s to reach room temperature, which facilitates a very rapid decrease from run temperatures at which melt is present to subsolidus conditions at 1100-900˚C to below the glass transition, which for these compositions is around 750˚C (Deubener et al., 2003).

This rapid quenching vastly improves quench structure for both hydrous and anhydrous silicate melts, allowing for improved quantification of melt compositions and facilitating better determination of the position of melting curves due to improved recognition of the presence of melts at low degrees of melting. This is particularly important for silica-undersaturated alkaline melts such as basanites, nephelinites, melilitites and kimberlites, which are known to originate in volatile-rich source regions. Crystals and overgrowths grown during the quench are minimised, lessening the confusion about interpretations of quenched melts, crystals and vapour which have, in the past led to controversy in the identification of rock solidi (Mysen and Boettcher, 1975; Till et al., Green et al., 2014).

Despite the many improvements a rapid-quench piston cylinder offers, access to them is currently limited as is the pressure-temperature range which they can achieve. Our comparison of melt compositions between RQPC experiments and those run in older apparatuses shows that accurate analyses can be achieved by EPMA analysis of quench-modified silicate glasses using defocused beams of at least 20 μm or integration of WDS measurements collected in grid patterns covering a minimum area of 100 μm^2. The resulting homogenised large area measurements are in good agreement with chemical compositions determined from RQPC experiments and can therefore be routinely used when determining glass compositions from quench-modified glasses.

Despite these improvements in quenching rates, further challenges lie ahead, most notably for carbonate-rich melts, which usually produce complex intergrowths of quench crystals with little or no glass preserved (Weidendorfer et al., 2020; Pintér et al., 2021).

For these, the development of the PiFM technique (Oddää et al., 2021) promises to make sense of nanoscale features, and may be assisted by a greater understanding of the stabilisation of amorphous carbonates as function of chemistry (e.g. Tester et al., 2014).

Authors contributions

I.S.E: Conceptualization (lead); writing – original draft (lead); formal analysis (lead); writing – review and editing (equal); methodology (lead). S.S.S: Methodology (supporting); formal analysis (supporting); writing – review and editing (equal). S.B: Conceptualisation (supporting); methodology (supporting); writing – review and editing (equal). A.B: conceptualisation (supporting); methodology (supporting). L.R.G: Resources (supporting); writing – review and editing (supporting). J.J.S: Resources (supporting); writing – review and editing (supporting). M.W.F: Conceptualisation (supporting); writing – original draft (supporting); writing – review and editing (equal), methodology (supporting). S.F.F. Conceptualisation (supporting); writing – original draft (supporting; writing – review and editing (equal), supervision (lead); funding acquisition (lead).

Acknowledgements

The prototype RQPC, designed by Stephan and Andreas Buhre, was built at the Geocycles Earth System Science Research Centre of the Johannes Gutenberg University of Mainz, funded by the State of Rhineland-Palatinate. The Macquarie instrument was funded by Macquarie University in support of the Australian Research Council Laureate Fellowship to SFF. The authors wish to thank Sean Murray for his help with imaging on the FE-SEM at Macquarie University and Sandrin Feig for his assistance with FE-EMPA data collection at the University of Tasmania.

AIP publishing data sharing policy

The data that supports the findings of this study are available within the article.

References

Boyd, F. R., England, J.L., 1960. Apparatus for phase-equilibrium measurements at pressures up to 50 kilobars and temperatures up to 1750°C. Journal of Geophysical Research 65, 741–748. https://doi.org/10.1029/JZ065i002p00741

Davis, F.A., Hirschmann, M.M., Humayan, M., 2011. The composition of the incipient partial melt of garnet peridotite at 3 GPa and the origin of OIB. Earth and Planetary Science Letters 308, 380-390.

Deubener, J., Müller, R., Behrens, H., Heide, G., 2003. Water and the glass transition temperature of silicate melts. Journal of Non Crystalline Solids 330, 268–273. https://doi.org/10.1016/S00223093(03)00472-1

Ezad, I.S, Foley, S.F., 2022. Experimental partitioning of fluorine and barium in lamproites. American Mineralogist, in Press. https://doi.org/10.2138/am-2022-8289

Foley, S.F., 1989. Experimental constraints on phlogopite chemistry in lamproites: 1. The effect of water activity and oxygen fugacity. European Journal of Mineralogy 1, 411–426. https://doi.org/10.1127/ejm/1/3/0411

Foley, S.F., Pintér, Z., 2018. Primary melt compositions in the Earth's mantle. In: (Kono, Y., ed.) Magmas under pressure, Elsevier, Amsterdam, pp. 3-42

Green, D.H., 1976. Experimental testing of "equilibrium" partial melting of peridotite under water-saturated, high-pressure conditions. Canadian Mineralogist 14, 255-268.

Green, D.H., Falloon, T.J., 1998. Pyrolite: a Ringwood concept and its current expression. In (Jackson, I., ed.) The Earth's mantle: composition, structure and evolution, Cambridge University Press, Cambridge, pp. 311-378.

Green, D.H., Hibberson, W.O., Rosenthal, A., Kovacs, I., Yaxley, G.M., Falloon, T.J., Brink, F., 2014. Experimental study of the influence of water on melting and phase assemblages in the upper mantle. Journal of Petrology 55, 2067-2096.

Grove, T.L., Chatterjee, N., Parman, S.W., Médard, E., 2006. The influence of H_2O on mantle wedge melting. Earth and Planetary Science Letters 249, 74-89.

Hess, P.C., 1977. Structure of silicate melts. Canadian Mineralogist 15, 162-178.

Hirose, K., Kushiro, I., 1993. Partial melting of dry peridotites at high pressures: Determination of compositions of melts segregated from peridotite using aggregates

of diamond. Earth and Planetary Science Letters 114, 477–489. https://doi.org/10.1016/0012-821X(93)90077-M

Holland, T.J.B., 1980. The reaction albite= jadeite+ quartz determined experimentally in the range 600-1200 degrees C. American Mineralogist 65, 129–134.

Ishii, T., Liu, Z., Katsura, T., 2019. A Breakthrough in Pressure Generation by a Kawai-Type Multi-Anvil Apparatus with Tungsten Carbide Anvils. Engineering. https://doi.org/10.1016/j.eng.2019.01.013

Jenei, Z., O'Bannon, E.F., Weir, S.T., Cynn, H., Lipp, M.J., Evans, W.J., 2018. Single crystal toroidal diamond anvils for high pressure experiments beyond 5 megabar. Nature Communications 9, 3563. https://doi.org/10.1038/s41467-018-06071-x

Kawai, N., Endo, S., 1970. The generation of ultrahigh hydrostatic pressures by a split sphere apparatus. Review of Scientific Instruments 41, 1178–1181. https://doi.org/10.1063/1.1684753

Masotta, M., Freda, C., Paul, T.A., Moore, G.M., Gaeta, M., Scarlato, P., Troll, V.R., 2012. Low pressure experiments in piston cylinder apparatus: Calibration of newly designed 25mm furnace assemblies to P=150MPa. Chemical Geology 312–313, 74–79. https://doi.org/10.1016/j.chemgeo.2012.04.011

Melekhova, E., Blundy, J., Martin, R., Arculus, R., Pichavant, M., 2017. Petrological and experimental evidence for differentiation of water-rich magmas beneath St. Kitts, Lesser Antilles. Contributions to Mineralogy and Petrology 172. https://doi.org/10.1007/s00410-017-1416-3

Mysen, B.O., Boettcher, A.L., 1975. Melting of a hydrous mantle: I. Phase relations of a natural peridotite at high pressures and temperatures with controlled activities of water, carbon dioxide and hydrogen. Journal of Petrology 16, 520-548.

Mysen, B.O., Virgo, D., Siefert, F.A., 1982. The structure of silicate melts; implications for chemical and physical properties of natural magma. Reviews of Geophysics 20, 353-383.

Otter, L.M., Förster, M.W., Belousova, E., O'Reilly, P., Nowak, D., Park, S., Clark, S., Foley, S.F., Jacob, D.E., 2021. Nanoscale Chemical Imaging by Photo-Induced Force

Microscopy: Technical Aspects and Application to the Geosciences. Geostandards and Geoanalytical Research 45, 5–27. https://doi.org/10.1111/ggr.12373

Parat, F. Streck, M.J., Holtz, F., Almeev, R., 2014. Experimental study into the petrogenesis of crystal-rich basaltic to andesitic magmas at Arenal volcano. Contributions to Mineralogy and Petrology, 168, 1040.

Perrillat, J.P., Daniel, I., Lardeaux, J.M., Cardon, H., 2003. Kinetics of the coesite-quartz transition: Application to the exhumation of ultrahigh-pressure rocks. Journal of Petrology 44, 773–788. https://doi.org/10.1093/petrology/44.4.773

Pintér, Z., Foley, S.F., Yaxley, G.M., Rosenthal, A., Rapp, R.P., Lanati, A.W., Rushmer, T., 2021. Experimental investigation of the compositon of incipient melts in upper mantle peridotites in the presence of CO_2 and H_2O. Lithos 396-397, 106224.

Tester, C.C., Whittaker, M.L., Joester, D., 2014. Controlling nucleation in giant liposomes. Chemical Communications 50, 5619.

Tiepolo, M., Vannucci, R., Oberti, R., Foley, S., Bottazzi, P., Zanetti, A., 2000. Nb and Ta incorporation and fractionation in titanian pargasite and kaersutite: crystal-chemical constraints and implications for natural systems. Earth and Planetary Science Letters 176, 185-201.

Till, C.B., Grove, T.L., Withers, A.C., 2012. The beginnings of mantle wedge melting. Contributions to Mineralogy and Petrology 163, 669-688.

Walker, D., Carpenter, M.A., Hitch, C.M., 1990. Some simplifications to multianvil devices for high pressure experiments. American Mineralogist 75, 1020–1028.

Wallace, M.E., Green, D.H., 1988. An experimental determination of primary carbonatite magma composition. Nature 335, 343-346.

Weidendorfer, D., Manning, C.E., Schmidt, M.W., 2020. Carbonate melts in the hydrous upper mantle. Contributions to Mineralogy and Petrology 175, 72.

Figure 1. The rapid quench piston cylinder apparatuses at Macquarie University. (a) Laboratory with two RQPC apparatuses; (b) close-up of one RQPC with experiment running; (c) Control panel with touch-screen programmable ramps for temperature and pressure; (d) Strecon pressure vessel with additional cooling channels close to the tungsten carbide core which improve cooling rate and core lifetime.

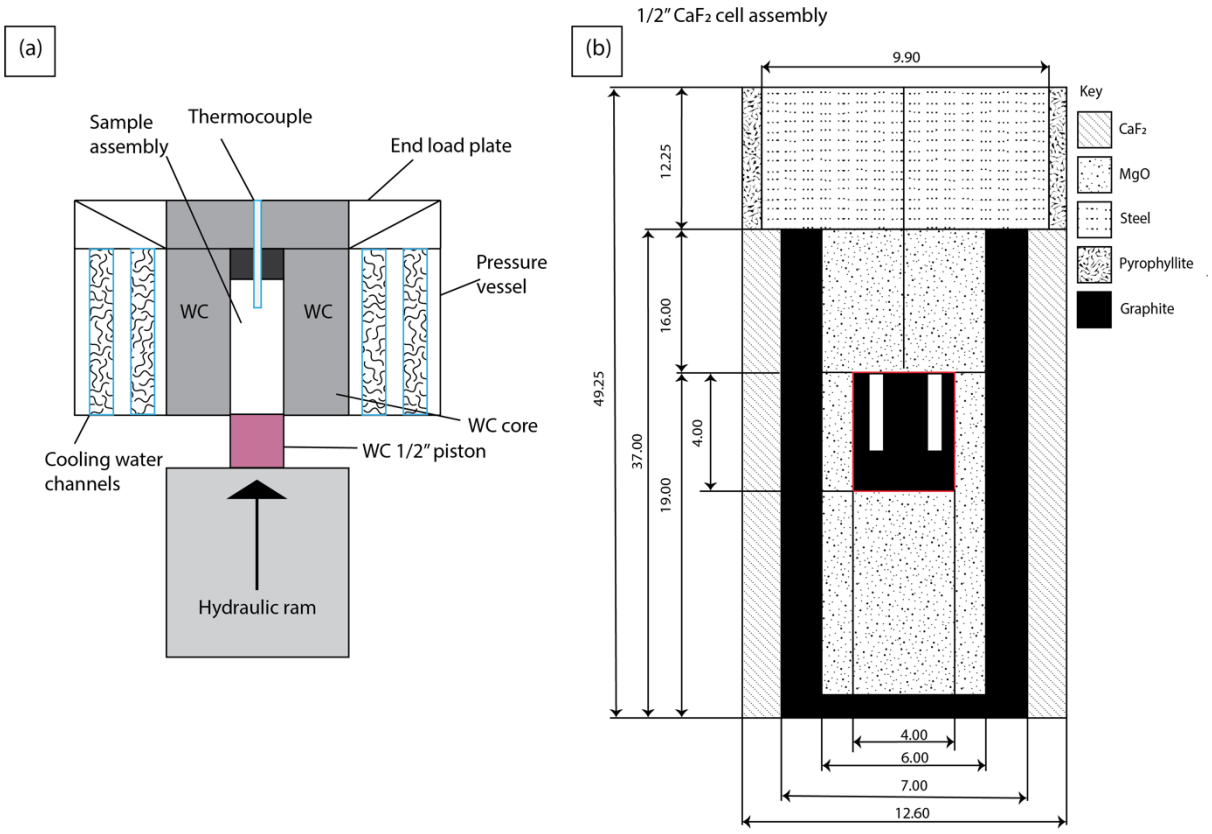

Figure 2. Schematic drawings of the RQPC pressure vessel and CaF_2 cell assembly used in high-pressure, high-temperature experiments. (a) Cross section of the pressure vessel with additional cooling water channels which help to rapidly cool the tungsten carbide core, rapidly quenching melts to glass upon cutting power to the furnace. (b) The standard ½" CaF_2 cell assembly used for experiments in the RQPC, graphite capsules wrapped in noble metals such as platinum are used with dual sample chambers to prevent iron loss. In some fluid bearing experiments welded Pt capsules are used to prevent fluid loss at high temperatures. The Pt capsules are pre-enriched in Fe to prevent iron loss during the experiments.

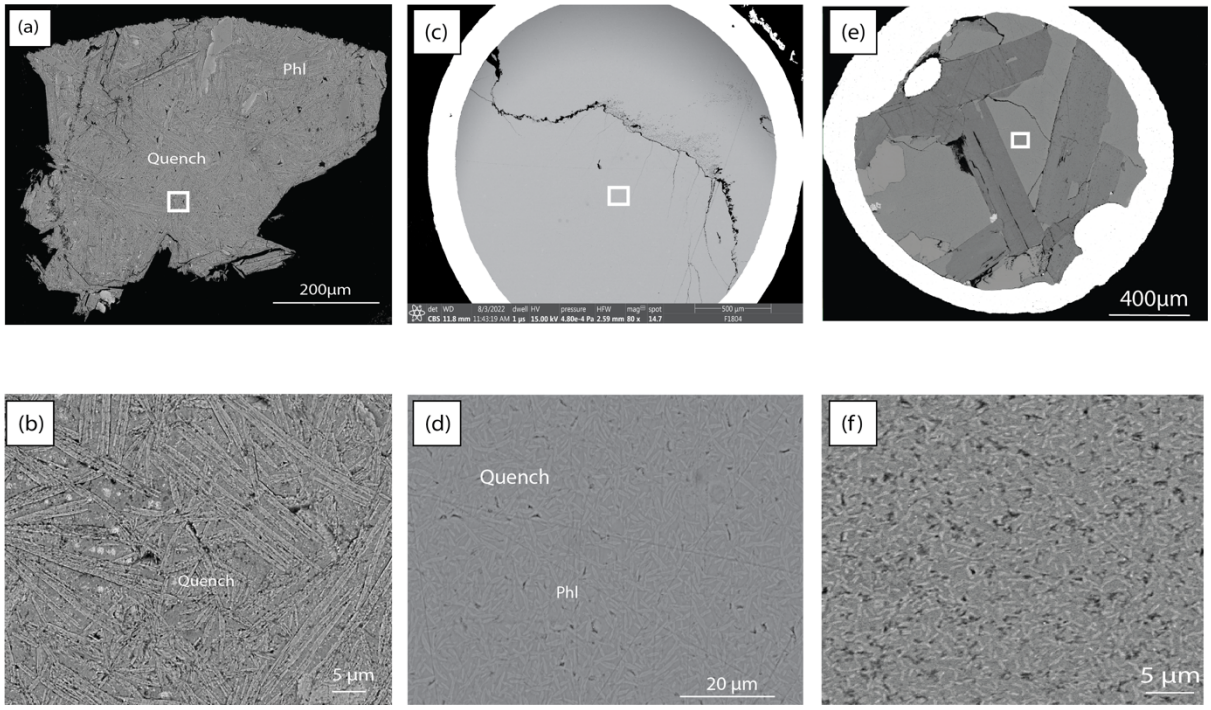

Figure 3. Back-scattered images of experimental charges recovered from high-pressure, high-temperature experiments on a synthetic hydrous leucite lamproite: a-d are experiments run in traditional piston cylinder apparatuses whilst e-f are those recovered from the rapid quench apparatus. (a) Experiment T1863 2.5 GPa, 1150°C with a CH_4<H_2O fluid. (b) High-magnification image of the area in the white box in (a). Substantial growth of quench phlogopite and orthopyroxene are present. (c) Experiment OLD-PC-212, 1.5 GPa, 1200°C with 5 wt% water. (d) High-magnification image of the quenched glass in the white box in (c): large ~10µm phlogopites that grew during the quench are present within the glass. (e) Experiment M21-059, 1.5 GPa, 1100°C, 5wt% H_2O, recovered from the rapid quench apparatus. Large phlogopites and clinopyroxenes were grown to facilitate a mineral-melt partitioning study (Ezad and Foley., in press). (f) High-magnification image of the quenched glass in the area in the white box in (e), Needles of quench crystals are dramatically smaller (< 1µm) compared to those in (d).

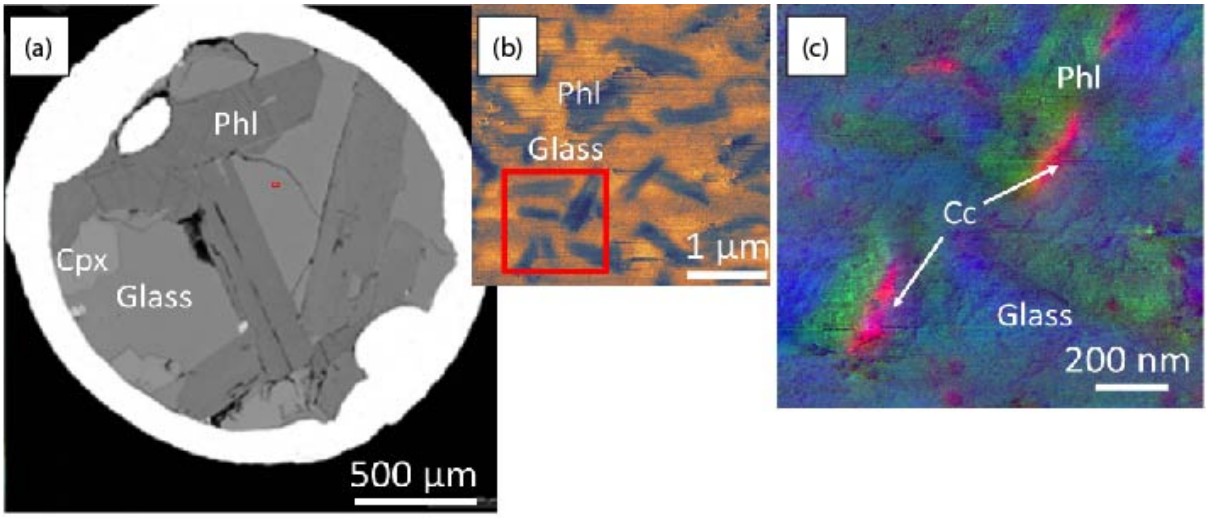

Figure 4. PiFM images of experiment M21-059 (synthetic lamproite with 5wt% H_2O). (a) Back-scattered image of experimental charge M21-059 showing position of PiFM images as red box. (b) PiFM map collected at wavenumber 1150 cm^{-1}, characterising silicate glass. Higher PiFM response is denoted by orange colour, with dark regions highlighting quenched phlogopite which are only 200nm in size. (c) PiFM map combining maps collected at 1000 cm^{-1} (ν_3 stretching vibration of Si-O of mica), 1150 cm^{-1} (ν_3 stretching vibration of Si-O of glass), and 1400-1450 cm^{-1} (ν_3 stretching vibration of C-O of carbonate) wavenumbers. The quenched melt (glass; blue) contains tiny quench phlogopite (Phl; green) and associated calcite (Cc; red), which demonstrates limited volatile loss from the melt during quenching. There are no other visible quench phases in experiment M21-059.

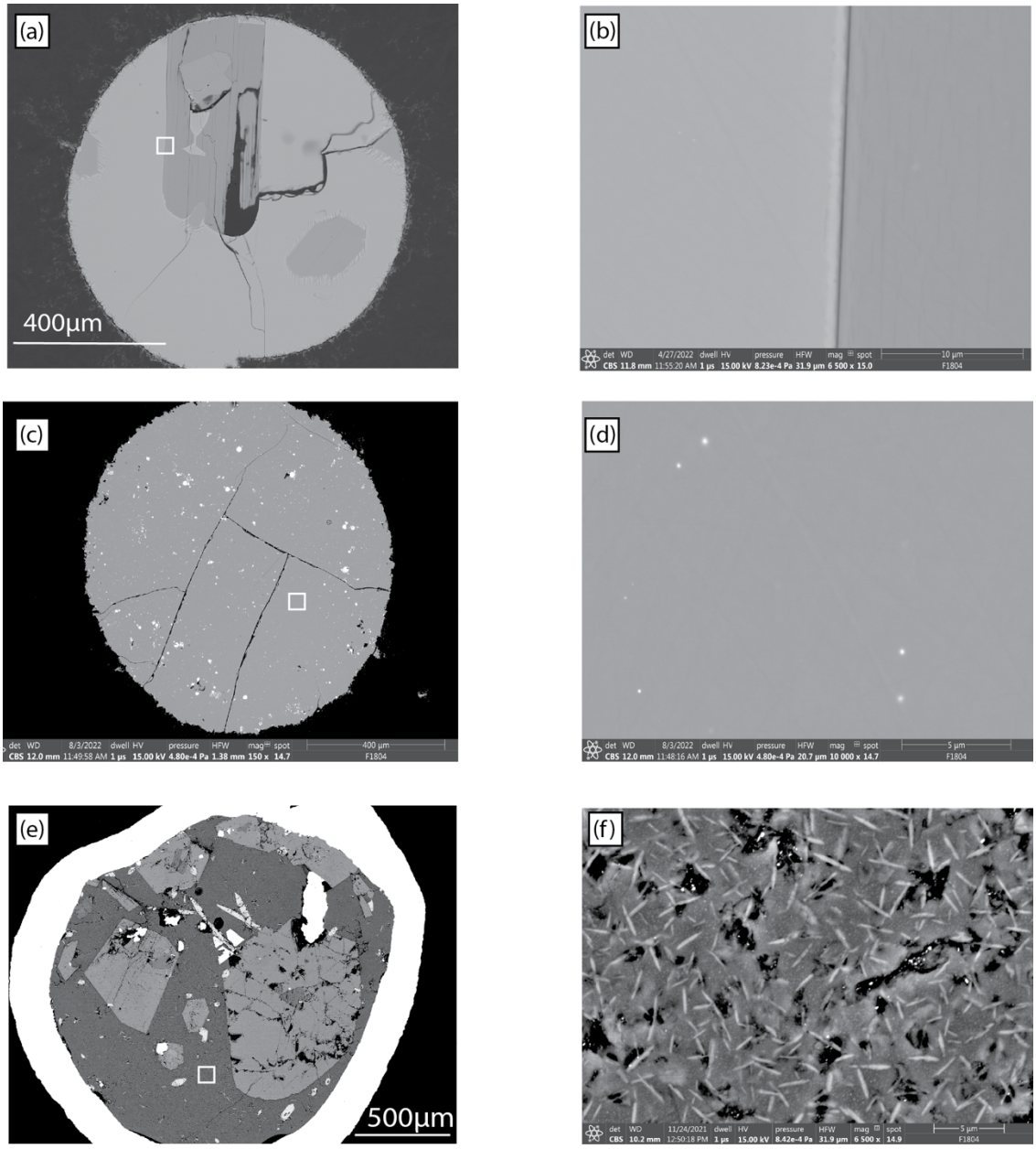

Figure 5. High-pressure, high-temperature experiments recovered from the rapid quench piston cylinder apparatus for a variety of compositions, pressures and temperatures. All experiments have large regions of silicate glasses with little to no visible quench crystal growth. (a) Experiment M22-027, low-Si lamproite, 1 GPa, 1200°C, 3 wt% H_2O. (b) High-magnification image of quenched glass from the white box in (a). There are no visible quench needles in this hydrous lamproite glass. (c) Experiment A21-028-A, tholeiite, 1 GPa, 1280°C. (d) High-magnification image of quenched glass in (c). (e) Experiment M21-104-B, basanite, 1 GPa, 975°C, 10 wt% H_2O. (f) High-magnification image of quenched glass in (e): only small (<1µm) phlogopite needles are present within the glass despite the high water content.

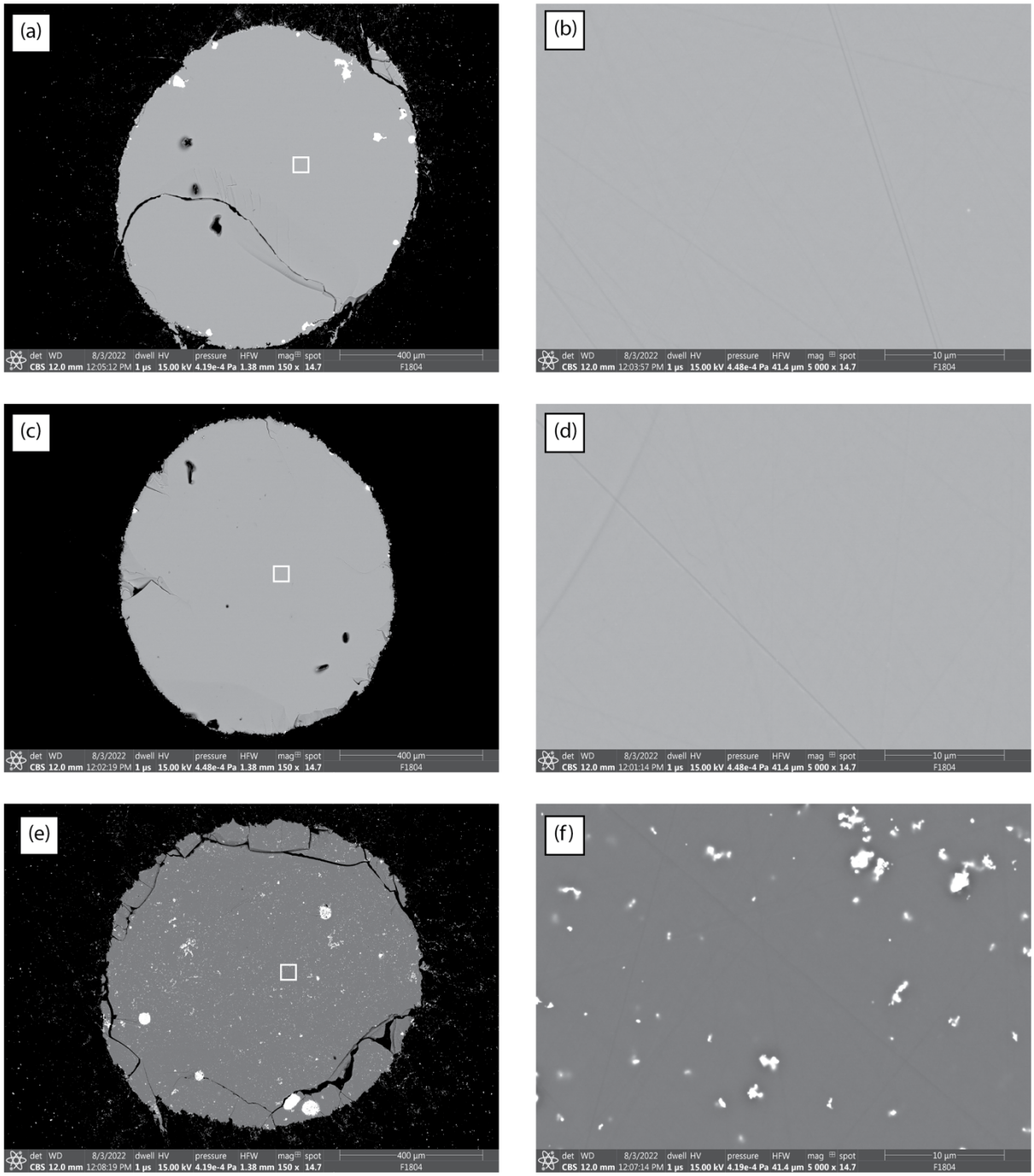

Figure 6. High-pressure, high-temperature experiments recovered from the rapid quench piston cylinder on calc-alkaline and tholeiite basaltic melts, with and without water. (a) Experiment A21-028-B, 1GPa, 1280°C – anhydrous tholeiite basalt. (b) High-magnification image of (a). (c) A21-035-A, calc-alkaline dacite, 1GPa, 1250°C, 5 wt% H_2O. (d) High-magnification image of (c). (e) Experiment A21-035-B, tholeiite basalt, 1GPa, 1250°C, 3.5 wt% H_2O. (f) High-magnification image of (e). Panels d and f are the same scale as b and show no quench crystal growth despite the addition of water.

Table 1. Composition of starting materials (wt%), determined by whole rock XRF.

	Gaussberg Leucite Lamproite (GL)	Leucite Lamproite (LL)*	Lake Cargelligo (LC)	Calc-alkaline dacite*	Tholeiite basalt*	Buckland basanite (BK-75115)
SiO_2	50.7	51.4	43.0	66.45	49.83	41.52
TiO_2	2.38	3.45	3.67	0.72	1.83	2.36
Al_2O_3	9.9	9.95	7.53	13.95	13.52	12.33
Cr_2O_3	0.08	0.1		0.0044	0.004	0.0226
FeO_{TOT}	5.97	6.1	8.97	4.75	14.85	13.85
MnO	0.09	0.09	0.14	0.13	0.230	0.21
NiO	0.03	0.03		0.00	0.430	0.0217
MgO	8.12	8.03	13.5	1.18	5.29	11.71
CaO	4.75	4.67	9.15	3.38	9.62	9.57
Na_2O	1.71	1.67	1.22	4.75	2.68	4.05
K_2O	11.53	11.76	7.39	1.66	0.093	1.65
BaO		0.63	0.65			
P2O5	1.45	1.5	0.86			1.34
F		0.33				
TE				2.30	0.930	
Sum	96.7	99.71	96.1	99.3	99.3	98.6

* asterisk denotes synthetic oxide mix

Table 2. Experimental compositions and run conditions

Run #	Composition	Pressure (GPa)	Annealing temperature (C)	Temperature (C)	Duration (hrs)	Water added (wt %)	Phases	Press type	Experimental aim	Capsule Type
T1863	LL	2.5		1150	24	*	Phl, Opx, Glass	Boyd and England	Melting experiments with controlled fluid	Dual graphite sample and buffer capsules in outer welded Pt
OLD-PC 212	GL	1.5	-	1200	0.5	5	Glass	Boyd and England	Glassing experiment	Welded Fe doped Pt capsule
M21 - 059	GL	1.5	1350	1100	24	5	Phl, Cpx, Glass	RQPC	Mineral-melt partitioning	Welded Fe doped Pt capsule
A21-063	GL	1.5	1400	1250	24	0	Glass	RQPC	Mineral-melt partitioning	Welded Fe doped Pt capsule
A21 - 028 - A	Calc-alkaline	1	-	1280	8	0	Glass	RQPC	Sulfur solubility	Dual sample chamber graphite capsule wrapped in Pt
A21 - 028 - B	Tholeitte basalt	1	-	1280	8	0	Glass	RQPC	Sulfur solubility	Dual sample chamber graphite capsule wrapped in Pt
M21 - 104 - B	BK--75115	1	1200	975	24	10	Amph, Phl, Ap, Glass	RQPC	Mineral-melt partitioning	Welded Fe doped Pt capsule
A21 - 035 - A	Calc-alkaline	1	-	1250	8	5	Glass	RQPC	Sulfur solubility	Dual sample chamber graphite capsule wrapped in Pt
A21 - 035 - B	Tholeitte basalt	1	-	1250	8	3.5	Glass	RQPC	Sulfur solubility	Dual sample chamber graphite capsule wrapped in Pt
M22 - 027	LC	1	1400	1200	24	0	Ol, Phl, Glass	RQPC	Mineral-melt partitioning	Dual sample chamber graphite capsule wrapped in Pt

*experiment contained a mixed CH4-H2O fluid consisting of 80% H2O and 20% CH4

"Annealing temperature refers to overheating of mineral/melt partitioning experiments above the liquidus, before slow cooling to target temperature and holding for the experimental duration

Table 3. Major element compostions of recovered experimental glasses as determined by EMPA (wt%)

Rock	T1863 high-Si lamproite H2O+CH4	OLD-PC 212 high-Si lamproite 5% H2O	M21 - 059 high-Si lamproite 5% H2O	A21 - 028 - A dacite anhydrous	A21 - 028 - B tholeiite anhydrous	M21 - 104 - B basanite 10% H2O	A21 - 035 - A dacite 5% H2O	A21 - 035 - B tholeiite 3.5% H2O	M22 - 027 low-Si lamproite no additional H2O added
n	25	8	4	5	5	5	5	5	5
SiO_2	50.88 (0.42)	48.69 (0.49)	52.36 (0.25)	66.27 (0.55)	49.06 (0.43)	49.05 (0.27)	65.91 (0.30)	51.39 (0.62)	45.69 (0.21)
TiO_2	3.16 (0.07)	3.09 (0.03)	3.2 (0.01)	0.64 (0.10)	1.65 (0.04)	1.22 (0.02)	0.75 (0.01)	1.7 (0.02)	3.88 (0.02)
Al_2O_3	10.20 (0.18)	8.95 (0.06)	9.34 (0.03)	14.35 (0.09)	13.86 (0.15)	16.28 (0.08)	14.34 (0.22)	14.29 (0.27	8.27 (0.06)
Cr_2O_3	0.09 (0.02)	0.05 (0.01)		0.11 (0.01)	0.13 (0.03)		0.13 (0.08)	0.12 (0.03)	0.07 (0.02)
FeO_{TOT}	5.17 (0.22)	4.44 (0.18)	2.57 (0.03)	3.79 (0.21)	12.61 (0.16)	5.84 (0.14)	4.73 (0.09)	14 (0.11)	6.21 (0.18)
MnO	0.07 (0.01)	0.09 (0.02)	0.12 (0/01)	0.11 (0.03)	0.22 (0.02)		0.17 (0.02)	0.22 (0.22)	0.13 (0.01)
NiO	0.02 (0.02)				0.06 (0.02)	0.26 (0.02)			
MgO	6.59 (0.40)	9.3 (0.15)	4.61 (0.09)	1.68 (0.13)	6.95 (0.13)	2.85 (0.12)	1.15 (0.02)	4.72 (0.07)	12.83 (0.04)
CaO	4.24 (0.32)	4.17 (0.06)	3.24 (0.08)	3.31 (0.16)	8.75 (0.10)	4.54 (0.13)	2.73 (0.05)	7.13 (0.03)	9.24 (0.03)
Na_2O	0.70 (0.14)	1.42 (0.13)	1.96 (0.02)	4.55 (0.18)	2.34 (0.04)	6.04 (0.89)	4.9 (0.09)	2.38 (0.06)	1.24 (0.03)
K_2O	7.78 (0.46)	10.26 (0.08)	11.59 (0.12)	1.88 (0.05)	0.26 (0.01)	2.36 (0.08)	1.93 (0.03)	0.22 (0.01)	6.37 (0.03)
BaO	0.50 (0.06)	0.61 (0.03)	0.79 (0.03)		0.07 (0.01)	0.10 (0.01)		0.06 (0.01)	0.63 (0.02)
P2O5	1.64 (0.07)	1.3 (0.02)	1.63 (0.03)			0.96 (0.03)			0.76 (0.02)
Cl		0.09 (0.01)	0.13 (0.01)			0.07 (0.01)			0.03 (0.01)
F	0.18 (0.02)	0.29 (0.01)	0.18 (0.01)			0.05 (0.02)			0.26 (0.01)
H2O*		7.25	8.28			10.00			4.51
SO3				0.10 (0.03)	0.22 (0.02)		0.11 (0.01)	0.21 (0.02)	
Sum	91.24	100	100	96.85	96.25	100.00	96.85	96.23	95.49

***H2O determined by difference from total**

Table 4 **Major element compostions of recovered experimental glasses as determined by EMPA (wt%)**

	T1863 high-Si lamproite H2O+CH4	OLD-PC 212 high-Si lamproite 5% H2O	A21-063 high-Si lamproite no additional water	Difference between OLD-PC 212 & A21-063 wt%
n	25	8	4	
SiO_2	50.88 (0.42)	48.69 (0.49)	50.45 (0.59)	-1.76
TiO_2	3.16 (0.07)	3.09 (0.03)	3.31 (0.09)	-0.22
Al_2O_3	10.20 (0.18)	8.95 (0.06)	9.69 (0.17	-0.74
Cr_2O_3	0.09 (0.02)	0.05 (0.01)	0.08 (0.01)	-0.03
FeO_{TOT}	5.17 (0.22)	4.44 (0.18)	4.86 (0.14)	-0.42
MnO	0.07 (0.01)	0.09 (0.02)	0.09 (0.01)	0
NiO	0.02 (0.02)			
MgO	6.59 (0.40)	9.3 (0.15)	9.56 (0.21)	-0.26
CaO	4.24 (0.32)	4.17 (0.06)	6.27 (0.14)	-2.1
Na_2O	0.70 (0.14)	1.42 (0.13)	1.32 (0.03)	0.1
K_2O	7.78 (0.46)	10.26 (0.08)	9.56 (0.19)	0.7
BaO	0.50 (0.06)	0.61 (0.03)	0.61 (0.04)	0
P2O5	1.64 (0.07)	1.3 (0.02)	1.26 (0.04)	-0.04
Cl		0.09 (0.01)	0.06 (0.01)	0.03
F	0.18 (0.02)	0.29 (0.01)	0.30 (0.02)	-0.01
H2O*		7.25	2.62	
SO3				
Sum	91.24	100	100	